

Temperature-induced sol-gel transition and microgel formation in α -actinin cross-linked actin networks: A rheological study

M. Tempel, G. Isenberg, and E. Sackmann

Department of Physics E22, Biophysics Group, Technische Universität München, James-Frank-Strasse, D-85747 Garching, Germany

(Received 15 April 1996)

We have studied the sol-gel transition, the viscoelastic and the structural properties of networks constituted of semiflexible actin filaments cross-linked by α -actinin. Cross-linking was regulated in a reversible way by varying the temperature through the association-dissociation equilibrium of the actin- α -actinin system. Viscoelastic parameters [shear storage modulus $G'(\omega)$, phase shift $\tan(\varphi)(\omega)$, creep compliance $J(t)$] were measured as a function of temperature and actin-to-cross-linker ratio by a magnetically driven rotating disc rheometer. $G'(\omega)$ and $\tan(\varphi)(\omega)$ were studied at a frequency ω corresponding to the elastic plateau regime of the $G'(\omega)$ versus ω spectrum of the purely entangled solution. The microstructure of the networks was viewed by negative staining electron microscopy (EM). The phase shift $\tan(\varphi)$ (or equivalently the viscosity η) diverges and reaches a maximum when approaching the apparent gel point from lower and higher temperatures, and the maximum defines the gel point (temperature T_g). The elastic plateau modulus G'_N diverges at temperatures beyond this gel point $T < T_g$ but increases only very slightly at $T > T_g$. The cross-linking transition (corresponding to a sol-gel transition at zero frequency) is interpreted in terms of a percolation model and the divergence of G'_N at $T < T_g$ is analyzed by a power law of the form $G'_N \sim [p(T) - p_c]^\gamma$ where $p(T)$ is the temperature dependent fraction of crosslinks formed. A power of $\gamma = 1.5 - 1.8$ is found. Negative staining EM shows (1) that the gel is essentially homogeneous above the cross-linking transition ($T > T_g$), (2) that microscopic segregation takes place at $T < T_g$ leading to local formation of clusters (a state termed microgel), and (3) that at low actin- α -actinin ratios ($r_{A\alpha} \leq 10$) and low temperatures ($T \leq 10^\circ\text{C}$) macroscopic segregation into bundles of cross-linked actin filaments and a diluted solution of actin filaments is observed. The three regimes of network structure are represented by an equivalent phase diagram. [S1063-651X(96)05408-6]

PACS number(s): 87.22.-q, 64.60.Ak, 64.75.+g, 83.80.Lz

I. INTRODUCTION

A central role of the actin network and the associated actin binding proteins for cell motility is now generally acknowledged (cf. [1]). However, the structural requirements (average chain length, degree of cross-linking) and the control mechanisms enabling the generation of stresses—ranging from some tenths to some hundreds of Pascals [2]—are largely unknown.

A prominent point of controversy arises from the mechanism driving the formation of cellular protrusions: Are these generated by the formation of strongly cross-linked actin bundles pushing the membrane forward? Or is the initial step determined by the formation of free volume between the actin cortex and the plasma membrane which is subsequently filled by a newly formed actin gel [3]?

A more physically motivated purpose of the present work is to show that the actin network provides a versatile model system to study fundamental properties of polymeric fluids and gels. Actin forms a living polymer consisting of double stranded semiflexible filaments [4]. The filaments (named F -actin) exhibit a fast (called barbed) and a slowly (called pointed) growing end. These different ends are due to the fact that the ratio of the association rate to the dissociation rate of monomeric actin (named G -actin, molecular weight 42 kDa) is large at the barbed end and small at the pointed end [5,6]. At steady state the rate of growth at the barbed end equals the rate of decay at the pointed end.

A large number of actin regulating proteins exist in a cell

[7,8]. To modify the actin network in a controlled manner we used the severing protein gelsolin and the cross-linking protein α -actinin. Binding of gelsolin to actin allows the adjustment of the actin filament length [9]. α -actinin is a homodimer with two actin binding sites. Depending on the concentration of bound α -actinin molecules this cross-linker tends to form random networks or bundles [10,11].

Since actin *in vitro* can form filaments up to 50 μm in length [12,13] networks exhibiting mesh sizes in the μm range can be generated, allowing the application of optical techniques (e.g., dynamic light scattering) to analyze internal conformational dynamics of the individual filaments [14,15]. Moreover single filament chains can be visualized by microfluorescence to investigate their bending undulations and reptation dynamics [16,17].

In the present study we have analyzed networks of actin filaments cross-linked by α -actinin. The association-dissociation equilibrium of the actin- α -actinin binding changes with temperature, i.e., by varying the temperature the degree of cross-linking can be continuously regulated in a reversible way. By lowering the temperature the networks can be driven from entangled (semidilute) solutions to the gel state (cf. [18]).

The viscoelastic impedance $G^*(\omega)$ [$= G'(\omega) + iG''(\omega)$] and the creep compliance $J(t)$ of actin- α -actinin networks for various actin-to- α -actinin molecular ratios were measured by a magnetically driven rotation disc rheometer (cf. [19,20]) as a function of temperature corresponding to a variation of cross-linking. The temperature range covered the

transition of the network from a sol state to a gel state (occurring at a gel point temperature T_g). The divergence of the elastic shear constant G'_N below the gel point $T < T_g$ is interpreted in terms of the percolation theory of viscoelasticity of gels.

Studies of these actin networks by negative staining electron microscopy (EM) provide evidence for a transition from a homogeneous gel state (with a mesh size corresponding to that of the purely entangled solution) to a microgel state which is heterogeneous on a μm scale but appears homogeneous on a macroscopic scale. At very low molar actin- α -actinin ratios ($r_{A\alpha} < 10$) complete phase separation into a highly dilute sol state and bundles of actin filaments could be observed.

Extending the recent rheological studies of Wachsstock, Schwartz, and Pollard [11,21], where gel formation of actin- α -actinin networks was studied by varying the α -actinin concentration and where data were analyzed in a qualitative way, we now give a quantitative interpretation.

II. MATERIALS AND METHODS

Buffers. The polymerization of actin was achieved in the usual way by adding physiological amounts of bivalent ions Mg^{2+} and Ca^{2+} to the aqueous solution in which the monomeric actin (called G -actin) was originally dissolved. The composition of the G buffer was: 2 mM Tris, 0.5 mM ATP, 0.2 mM CaCl_2 , 0.2 mM dithiothreitol, 0.005 vol% NaN_3 at pH 7.4. The composition of the actin polymerizing buffer (called F buffer) was: 2 mM Imidazol, 0.5 mM ATP, 100 mM KCl, 2 mM MgCl_2 , 0.2 mM CaCl_2 , 0.2 mM dithiothreitol at pH 7.4.

Proteins. Actin ($M_w = 42$ kDa) was extracted from an acetone powder of rabbit skeletal muscle according to Pardee and Spudich [22] with a gel filtration step as suggested by MacLean-Fletcher and Pollard [23] using a Sephacryl S-300 HR column. To minimize the fraction of residual actin binding proteins actin was only taken from the region beyond the elution peak. The concentration of G -actin was determined by absorption spectroscopy assuming an extinction coefficient of $0.63 \text{ mg}^{-1} \text{ ml}^{-1}$ for the absorption at 290 nm [24]. The ability of G -actin to polymerize was tested by the technique of falling ball viscometry as described by Pollard and Cooper [25]. Actin was stored in G buffer at 4 °C and was used within 10 days.

α -actinin ($M_w = 200$ kDa dimer) was prepared from smooth muscle of turkey gizzard as described by Craig, Lancashire, and Cooper [26]. The α -actinin concentration was determined by its absorption at 278 nm using an extinction coefficient of $0.97 \text{ mg}^{-1} \text{ ml}^{-1}$.

Gelsolin ($M_w = 82$ kDa) was purified from bovine plasma serum using a procedure based on that of Cooper *et al.* [27]. The concentration of gelsolin was determined by the Bradford technique with bovine serum albumin (BSA) as standard [28]. Before use, α -actinin and gelsolin were dialyzed for 18–24 h against G puffer and then stored at 4 °C for several weeks. The purity of the proteins was checked by SDS-polyacrylamide-gel-electrophoresis stained with comassie blue [29], and estimated to be at least 95%.

Rotation disc rheometer. The apparatus has been described in detail by Müller *et al.* [19]. The dynamic storage

and loss modulus $G'(\omega)$ and $G''(\omega)$ and the creep compliance $J(t)$ can be measured between $\omega/2\pi = 10^{-5} - 10^1$ Hz and $t = 10^{-1} - 10^4$ s, respectively. From the dynamic moduli the phase shift angle $\tan(\varphi)$ can be calculated as $\tan(\varphi) = G''/G'$.

Basically, the rheometer consists of a cylindrical glass cuvette with a diameter of 15 mm and a volume of ≈ 1.5 ml. The base of the cuvette is mounted in an aluminum thermostated holder, which is in thermal contact with the solution. Temperature control is achieved by Peltier elements situated in the holder. A glass disc of diameter 8 mm is placed on the surface of the viscoelastic solution. On top of the disc a magnet with dimensions of $0.5 \times 0.5 \times 1.5 \text{ mm}^3$ and a $1.5 \times 2.0 \text{ mm}^2$ deflection mirror are mounted; the plane of the latter forming an angle of 45° with the horizontal line.

The glass cuvette is surrounded by two perpendicularly oriented magnetic coils. One of these serves to fix the orientation of the disc and the other (the deflection coils) to apply shear forces to the viscoelastic liquid. The voltage of the deflection coils is computer controlled. For the measurements of the dynamic moduli $G'(\omega)$ and $G''(\omega)$ the deflection coils are driven with an oscillatory voltage of frequency ω . At measurements of the compliance $J(t)$ a constant voltage is applied to these coils. The magnetic coils and the measuring cuvette are placed within a μ -metal chamber to shield external (interfering) magnetic fields.

The rotational amplitude $\alpha(t)$ of the disc is analyzed as follows: The beam of a He-Ne laser incident in a vertical direction along the rotational axis of the disc is horizontally deflected by the mirror mounted on the disc. Its horizontal orientation is recorded by a position-sensitive photodiode. The amplified response of the diode is evaluated by computer.

The actin solution in the measuring cuvette is covered by a phospholipid monolayer (dimyristylphosphatidylcholine) which is essential to avoid the gelation of actin owing to its denaturation at the air-water interface [19]. Moreover, it ensures good mechanical contact to the glass disc which is covered by a monolayer of octadecyltrichlorosilane. Appropriate protein mixtures (400 μl total volume) were placed in the rheometer cuvette and were polymerized for 14–18 h before measurement.

Electron microscopy. Samples to be inspected by electron microscopy were absorbed to glow-discharged carbon-coated formvar films on copper grids for 60 s. The grids were washed with some drops of distilled water. Excess liquid was drained with filter paper, and the grids were negatively stained with 0.8% uranyl acetate for 60 s. Excess liquid was again drained with filter paper.

III. RESULTS

The following three types of viscoelastic experiments were performed:

(i) In order to evaluate the time dependence of semidilute actin solutions or actin gels we measured the creep compliance $J(t)$ [30]. The transient function $J(t)$ gives more reliable values for the long time behavior of the viscoelasticity of the network than the usually measured values of the dynamic moduli $G'(\omega)$ and $G''(\omega)$.

(ii) To observe the temperature induced sol-gel transition

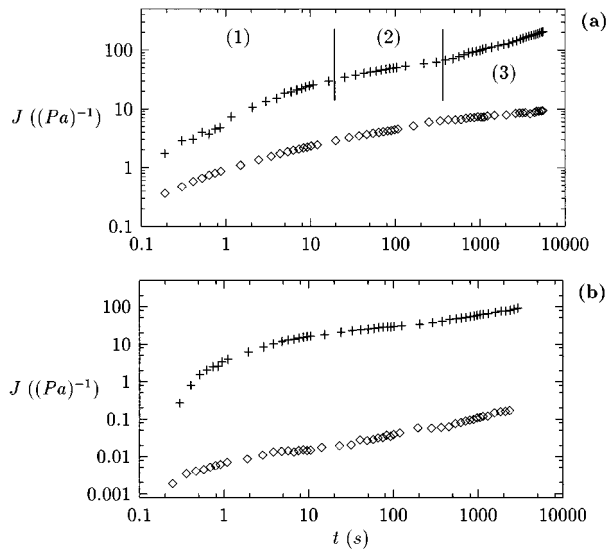


FIG. 1. Time dependence of creep compliance $J(t)$ of actin- α -actinin networks at temperature well above and well below the gel point. The average contour length of actin was controlled by adding gelsolin (copper molecule). The actin concentration was $c_A=9.5 \mu\text{mol}$ ($400 \mu\text{g/ml}$) exhibiting a mesh size of $\xi \approx 0.55 \mu\text{m}$. (a) Network of long chains. Actin-gelsolin molar ratio was $r_{AG}=8000$, corresponding to an average contour length of $\bar{L}=r_{AG} \times 2.8 \text{ nm} \approx 22 \mu\text{m}$. Actin-to- α -actinin molar ratio $r_{A\alpha}=55$. (\diamond): 5°C and ($+$): 25°C . The numbers indicate characteristic regimes for entangled actin solutions: (1) internal chain conformation dynamics, (2) rubber plateau, and (3) transition into fluidlike behavior. (b) Network of short chains. $r_{AG}=2000$, corresponding to $\bar{L} \approx 5.6 \mu\text{m}$. Actin-to- α -actinin molar ratio $r_{A\alpha}=10$. (\diamond): 10°C and ($+$): 25°C .

in a continuous way, the shear elastic constant G'_N was measured while the temperature was varied in the range between 6°C and 25°C . The measurement of G'_N was performed at a frequency of $\omega/2\pi=3.5 \times 10^{-3} \text{ Hz}$ corresponding to the plateau regime of the elastic modulus $G'(\omega)$.

(iii) Simultaneously with G'_N the phase shift $\tan(\varphi)$ was recorded as a function of temperature.

Figure 1 shows two examples of the time dependence of the compliance $J(t)$ of actin- α -actinin networks at a temperature well above and well below the gel point. The actin monomer concentration was $c_A=9.5 \mu\text{mol}$ corresponding to a mesh size of the purely entangled solution ($T \rightarrow \infty$) of $\xi \approx 0.55 \mu\text{m}$ [14]. The average contour length \bar{L} of the filaments was adjusted to $\bar{L} \approx 22 \mu\text{m}$ in Fig. 1(a) and to $\bar{L} \approx 5.6 \mu\text{m}$ in Fig. 1(b) by addition of appropriate amounts of gelsolin. The contour length and the end-to-end distance are thus at least one order of magnitude larger than the mesh size.

Above the gel point, [cf. Fig. 1(a), $+$], the $J(t)$ curve exhibits three regimes characteristic of entangled actin solutions [20]: a zone determined by the internal chain conformation dynamics (1), a rubber plateau in the center (2), and a terminal transition into fluidlike behavior (3).

A remarkably different behavior of the networks is observed below the gel point besides the shift of the curves to lower values of $J(t)$ (Fig. 1, \diamond):

The gel formed by the long chains, Fig. 1(a), shows saturation behavior at long times ($t \approx 10^4 \text{ s}$) as expected for a

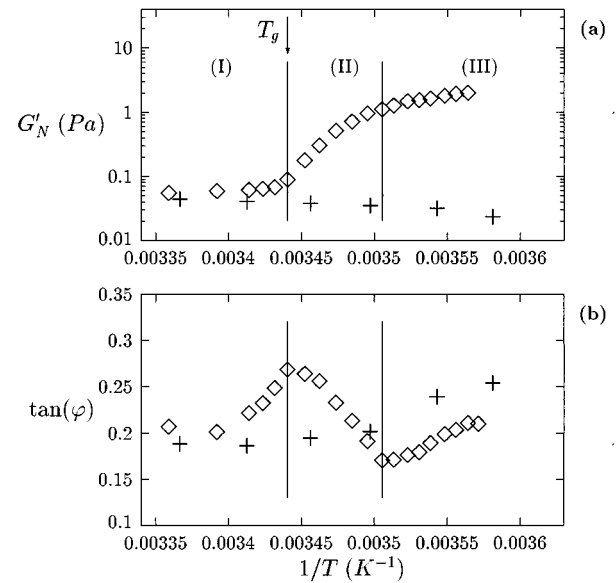


FIG. 2. (a) Arrhenius-like representation of shear elastic plateau modulus G'_N measured at the frequency $\omega/2\pi=3.5 \times 10^{-3} \text{ Hz}$ for an actin- α -actinin network (\diamond) and comparison with behavior of purely entangled actin solution ($+$). The average contour length of actin filaments was adjusted to $\bar{L} \approx 22 \mu\text{m}$ by adding gelsolin ($r_{AG}=8000$). The actin monomer concentration was $c_A=9.5 \mu\text{mol}$ and the actin-to- α -actinin molar ratio was $r_{A\alpha}=10$. (b) Arrhenius-like plot of phase shift angle $\tan(\varphi)$ simultaneously measured with G'_N for the same network as described in (a). The temperature was varied from 6°C to 25°C . The temperature, where G'_N starts to increase abruptly and where $\tan(\varphi)$ exhibits a maximum, is denoted as the apparent gel point temperature T_g (see vertical arrow). The roman numbers and vertical bars indicate regimes discussed in the text.

homogeneous network cross-linked over macroscopic dimensions. It appears, however, that a small finite slope of the $J(t)$ versus t curve remains, which could be attributed to the dissociation kinetics of the actin- α -actinin binding. In fact, the rate of dissociation of the cross-links is about 0.4 s^{-1} at 20°C [31] and the filaments could thus slowly slide past each other under a constant force due to the statistical breaking of actin- α -actinin bonds. Another explanation for the finite slope of $J(t)$ may be the fracture of actin filaments corresponding to shear thinning [32,33].

The more strongly cross-linked gel composed of shorter chains Fig. 1(b) exhibits a plateau at $t \approx 20 \text{ s}$ but shows fluidlike behavior at times $t > 10^2 \text{ s}$. This is explained in terms of a heterogeneous structure of the gel. As will be shown below, one can recognize in electron micrographs of the same sample a phase separation into a dilute sol state of actin filaments and a dense gel state of cross-linked actin filaments.

In Fig. 2(a) we show a typical example of the temperature dependence of the shear modulus observed by varying the temperature over the regime of the sol-gel transition. An Arrhenius-like plot of $\ln G'_N$ versus $1/T$ is presented, where T is the absolute temperature. The behavior of a purely entangled actin solution of the same concentration and the same average contour length is also shown. Figure 2(b) displays the Arrhenius-like plot of the phase angle $\tan(\varphi)$ of the

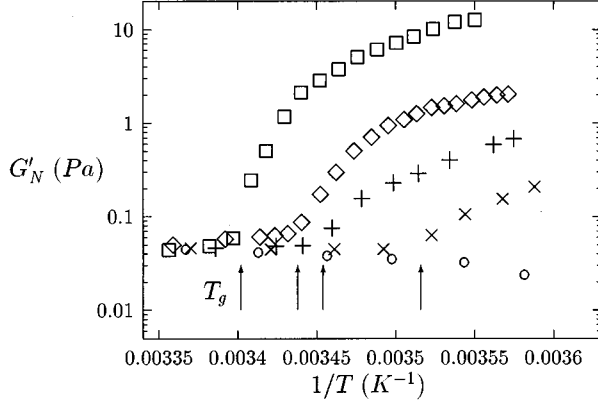


FIG. 3. Arrhenius-like representation of shear elastic plateau modulus G'_N measured at the frequency $\omega/2\pi=3.5\times 10^{-3}$ Hz for actin- α -actinin networks of different actin- α -actinin molar ratios. The actin monomer concentration, $c_A=9.5$ μmol , and the average contour length of the filaments $\bar{L}\approx 22$ μm ($r_{AG}=8000$), were the same in all cases. The actin- α -actinin molar ratios were (○) no crosslinker, (×) $r_{A\alpha}=55$, (+) $r_{A\alpha}=27$, (◇) $r_{A\alpha}=20$ and (□) $r_{A\alpha}=10$. The measurements were performed by increasing the temperature in the range 6–25 °C. The vertical arrows define the sol-to-gel transition temperature T_g for each data set (see Table I).

same actin network both in the absence and in the presence of the cross-linker.

A closer inspection of Fig. 2(b) reveals that one can distinguish three zones: At zone (I) the phase $\tan(\varphi)$ increases strongly with decreasing temperature whereas the elastic modulus G'_N increases only slightly but remarkably. At zone (II) G'_N increases steeply while $\tan(\varphi)$ decreases. Finally at zone (III) the values of G'_N and $\tan(\varphi)$ increase simultaneously. In the following we will denote the temperature where $\tan(\varphi)$ exhibits a maximum and where G'_N starts to increase abruptly as the apparent gel point or sol-to-gel transition temperature T_g . We use the term apparent since T_g may appear at a slightly different position than the gel point temperature which is obtained by measuring the zero shear viscosity.

In Fig. 3 a whole series of G'_N versus $1/T$ plots of actin- α -actinin networks of different actin-to- α -actinin molar ratios is presented. The various data sets essentially exhibit the same regimes described in Fig. 2. The divergence of G'_N at the sol-to-gel temperature ($T\leq T_g$) becomes less pronounced with increasing actin-to- α -actinin ratios, but can be clearly recognized in all cases. T_g is shifted to lower temperature with increasing value of $r_{A\alpha}$, see Table I. By plotting T_g against $r_{A\alpha}$ (not shown) a straight line is found, indicating a linear relationship between T_g and $r_{A\alpha}$.

In order to test the reversibility of the temperature-

TABLE I. Variation of temperature of gel point T_g with actin- α -actinin molar ratio $r_{A\alpha}$. Data taken from Fig. 3.

$r_{A\alpha}$	10	20	27	55
T_g^{-1} (10^{-3} K $^{-1}$)	3.402	3.438	3.454	3.516
T_g (°C)	20.9	17.9	16.5	11.4

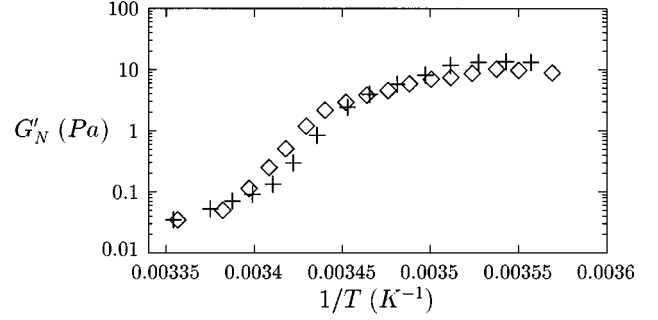


FIG. 4. On reversibility of temperature induced sol-gel transition. Measurements of G'_N versus $1/T$ for two actin- α -actinin networks of identical composition ($c_A=9.5$ μmol , $r_{AG}=8000$, $r_{A\alpha}=10$) at increasing (◇) and decreasing (+) temperature. (◇) Sample prepared at 6 °C and then measured from 6 °C up to 25 °C. (+) Sample prepared at 25 °C and then measured from 25 °C down to 8 °C. The rate of temperature change was about 2.5 °C/h in both directions.

induced sol-gel transition measurements were performed with increasing and decreasing temperature. Two samples of identical composition ($c_A=9.5$ μmol , $r_{AG}=8000$, $r_{A\alpha}=10$) were prepared where one sample was polymerized at low temperature, $T=6$ °C, and the other sample at high temperature, $T=25$ °C. The plateau modulus G'_N was measured at increasing temperatures in the former case and at decreasing temperatures in the latter case. As shown in Fig. 4 the G'_N versus $1/T$ plots agree well. At the steep ascent the two curves are shifted to each other by only ≈ 0.9 °C.

The microstructure of the networks was observed by negative staining electron microscopy. Although artifacts cannot be excluded during the drying process (cf. Sec. II) the technique yields at least qualitative images of the homogeneity and the average mesh size of the networks.

In Fig. 5 we present three micrographs for a sample with the composition $c_A=9.5$ μmol , $r_{AG}=8000$, and $r_{A\alpha}=10$ which were taken above ($T=30$ °C), just below ($T=19$ °C) and below ($T=10$ °C) the gel point ($T_g=20.9$ °C, see Table I). The mesh size of the purely entangled solution ($T\rightarrow\infty$) is calculated as $\xi\approx 0.55$ μm .

At 30 °C [Fig. 5(a)] one can recognize a homogeneous network with a mesh size corresponding to that of the purely entangled solution. At 19 °C [Fig. 5(b)] the network exhibits slight fluctuations in density whereas at 10 °C [Fig. 5(c)] strong fluctuations can be observed. However, in the two latter cases the networks are homogeneous on a macroscopic scale (micrographs not shown). It should be noted that for the given composition, $T=19$ °C is very near to the sol-to-gel transition temperature, $T_g=20.9$ °C. Therefore the spatial fluctuations in density are attributed to local segregations caused by the cross-linker. This indicates that the average distance between the cross-links near the gel point is smaller than the mesh size.

IV. DISCUSSION

The gelation of the actin networks may be effected in two ways: (a) by copolymerization of actin and cross-linker or

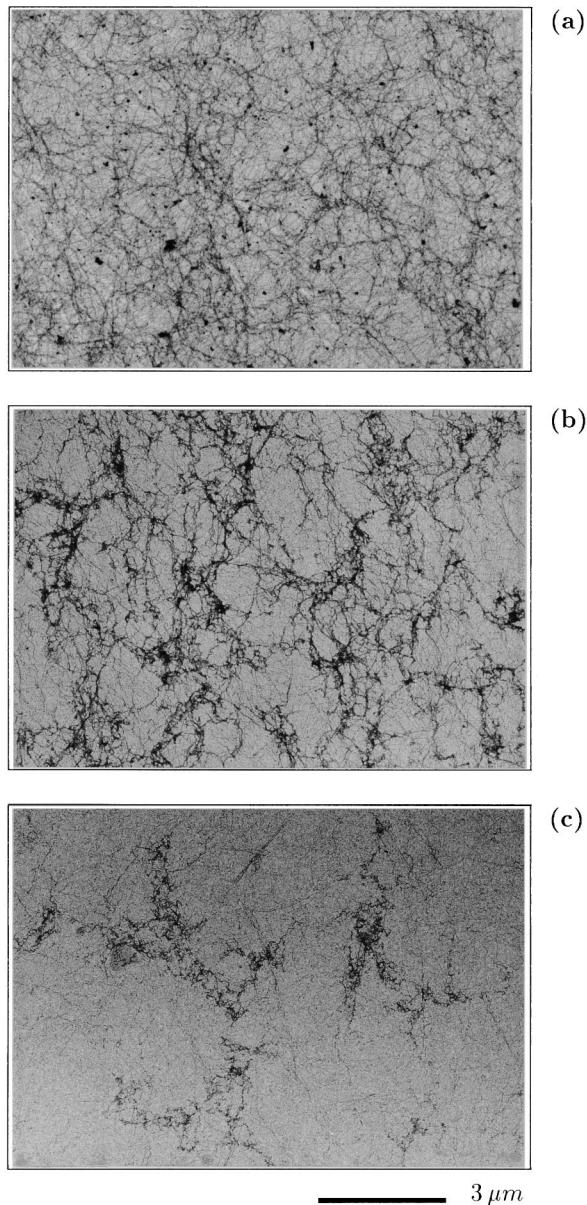


FIG. 5. Negative staining electron micrographs of an actin- α -actinin network ($c_A=9.5 \mu\text{mol}$, $r_{AG}=8000$, $r_{A\alpha}=10$) at three temperatures. The sol-gel transition temperature for the given composition was $T_g=20.9 \text{ }^\circ\text{C}$ (see Table I). (a) Temperature above sol-gel transition $T=30 \text{ }^\circ\text{C}$. (b) Temperature just below sol-gel transition $T=19 \text{ }^\circ\text{C}$. (c) Temperature below sol-gel transition $T=10 \text{ }^\circ\text{C}$. The bar represents $3 \mu\text{m}$.

(b) by polymerizing the actin filaments first while the cross-linker is activated subsequently. In the former case a locally heterogeneous gel forms, consisting of clusters of cross-linked short chains which are interconnected by long chains [34]. This structure is a consequence of the slow generation of actin trimers which are necessary as nuclei for the polymerization process [35]. It leads to the initial formation of very long chains which cannot effectively link due to their semiflexibility. At later times shorter chains are formed which are both cross-linked among themselves and coupled to long chains. Because of the fast diffusion of the short chains the gelation is associated with local phase separation. A microgel composed of clusters of interconnected short

chains coupled by long filaments results, which can be characterized by a small and a large value of the mesh size.

For the present experimental conditions the situation is much simpler because of the reversibility of the binding of actin and α -actinin. The protein gelsolin facilitates nucleation and leads to a nearly homogeneous length distribution of actin filaments [9]. Even if the gel is formed by copolymerization of actin and α -actinin at low temperatures and is thus heterogeneous, heating up well above the gel point and annealing for some hours will lead to a purely entangled, homogeneous solution which can then be gradually cross-linked by lowering the temperature.

The electron microscopic studies provide strong evidence that the gel is homogeneous at low degree of cross-linking [see Fig. 5(a)] corresponding to regime I in Fig. 2. The network assumes a slightly heterogeneous structure near the gel point [see Fig. 5(b)], where the phase $\tan(\varphi)$ has a maximum [see Fig. 2(b)]. The clusters of more densely packed and more strongly cross-linked filaments grow with decreasing temperature. This coarsening behavior is attributed to regime II in Fig. 2. However, even in this regime the gel is still homogeneous on a macroscopic scale. At very low temperature and high degree of cross-linking complete separation into bundlelike structures and dilute solution of residual filaments occurs. This conformation of the gel can basically be recognized in Fig. 5(c) and is attributed to regime III in Fig. 2. In the following we attempt to explain the sol-gel-like transition and the cluster formation in terms of a percolation model.

Percolation model of temperature induced sol-gel transition. The transition from a homogeneous state (Fig. 2, regime I) into the microheterogeneous state (Fig. 2, regime II) at increasing degree of cross-linking is well known from synthetic gels [36,37]. If the spatial density of the reacted cross-linkers is smaller than the density of the points of entanglement, cross-links are preferentially formed at the natural points of entanglement without changing the conformation of the polymers. With increasing number of cross-links, interconnected clusters of cross-linked points of entanglement are formed. The building of these clusters is equivalent to a bond percolation problem.

The size of the clusters grows with the fraction of α -actinin reacted. If the average distance of cross-links along the actin filaments becomes equal to the mesh size all points of entanglement are fixed. This point can (approximately) be attributed to the gel point T_g . Increasing the cross-linker density beyond the gel point ($T < T_g$) causes local contractions of the actin filaments and the spatial filament distribution becomes heterogeneous. The coarsening of the gel could imply increases of the amplitudes as well as of the correlation lengths of the density fluctuations (similar to the situation during spinodal decomposition).

The sharp rise of the elastic modulus at $T < T_g$ is not completely analogous to the situation of gel formation in solutions of short chains which are fluid prior to cross-linking. In our case it is due to the percolation transition of more densely packed cross-linked regions. The forming of spatial fluctuations in the polymer density has previously been observed in synthetic gels by small angle neutron scattering and can be described in terms of a percolation model if the cross-links are randomly formed [38]. Colby, Gillmor,

and Rubinstein [39] studied the viscoelasticity of gels (of the first kind) in the region of the sol-gel transition and showed that these properties can be well explained in terms of percolation but also in terms of mean field theory of critical phenomena and phase transitions. Following these authors we now attempt to explain our experimental data in terms of a percolation model.

The degree of cross-linking is characterized by the actual fraction of cross-links p formed during the reaction relative to the critical p -value p_c at which an infinite cluster of connected filaments is formed. The percolation theory of viscoelasticity of gels predicts two power laws (cf. [36,40,41]):

(i)

$$G'_N \sim (p - p_c)^t, \quad (1)$$

for the elastic constant G'_N at values $p > p_c$ (that means beyond the gel point), and

(ii)

$$\eta \sim (p_c - p)^{-s}, \quad (2)$$

for the viscosity η at values upon approaching the gel point from both sides (i.e., $p > p_c$ and $p < p_c$).

The exponents t and s depend on the theoretical model. The classical prediction by the mean field theory assuming an analogy between gels and electrical networks is $t = 1.7 - 1.9$ and $s = 1.3$ [36]. The more advanced percolation theories predict that close to the gel point the elastic constant of the system vanishes with $t \approx 3.8$ and the viscosity diverges with an exponent $s \approx 0.74$ [40].

In our study of the thermally induced gelation process we measured the elastic impedance $G^*(\omega)$ at a frequency of $\omega/2\pi = 3.5 \times 10^{-3}$ Hz and instead of η we measured the phase shift angle $\tan(\varphi)$, which is given by

$$\eta(\omega) = \omega G'' = \omega G' \tan(\varphi). \quad (3)$$

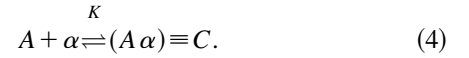
Due to the limited stability of the biopolymers (e.g., denaturation) it was not possible to measure the zero shear viscosity [e.g., by $J(t)$ versus t measurements], for which Eq. (2) strictly applies: because of the large filament length the measurement for each temperature would take 1–2 h. Moreover, the dynamic viscosity $\eta(\omega)$ is more interesting from the biological point of view since many chemomechanical processes of cells occur at the time scale of seconds.

The divergence of the viscoelastic parameters at the sol-gel transition is clearly revealed by the phase shift angle $\tan(\varphi)$: following Eq. (2) and Eq. (3), $\tan(\varphi)$ diverges at the gel point since the viscosity η diverges. The maximum of the $\tan(\varphi)$ versus $1/T$ plot, see Fig. 2(b), is thus attributed to the gel point.

The maximum of η can be explained by the postulate that the viscosity is determined by the time it takes a cross-linked cluster to diffuse over a distance equal to the cluster size. Since the percolation theory predicts that the size of the largest branched polymer diverges as the gel point is approached, the viscosity η [as well as phase shift $\tan(\varphi)$] assumes a maximum at the gel point from either side. The decrease of η beyond the gel point is attributed to the decrease of the cluster size caused by the local contraction of the network during microgelation.

A closer inspection of Fig. 2(a) and Fig. 3 also shows a slight but significant increase of G'_N at $p < p_c$ (i.e., $T > T_g$) with respect to the purely entangled solution. This difference can be attributed to the fixation of dangling bonds.

For a more qualitative evaluation of the behavior of G'_N at the sol-gel transition we have to consider the association-dissociation equilibrium of the complex formation between actin (A) and α -actinin (α)



K is the equilibrium constant of the reaction (in units of mol^{-1}) and is given by

$$K = \frac{[C]}{[A][\alpha]}, \quad (5)$$

where the square brackets denote concentrations (in units of mol).

The fraction of reacted α -actinin molecules is

$$\rho_\alpha = \frac{[C]}{[C] + [\alpha]} = \frac{[A]K}{[A]K + 1} \quad (6)$$

and since α -actinin is bifunctional the fraction of cross-links formed is

$$p = \frac{1}{2} \rho_\alpha. \quad (7)$$

Consider now the temperature dependence of the fraction of cross-links formed. Similar to Van't Hoff's law we use the relation

$$K = K_0 \exp\left(\frac{\Delta H}{RT}\right), \quad (8)$$

where K_0 is the equilibrium constant at some standard state, ΔH is the heat of association, and R is the gas constant. According to this equation the equilibrium (or association) constant K increases with decreasing temperature. Insertion of Eq. (8) into Eq. (6) yields for the fraction of cross-links formed Eq. (7)

$$p(T) = \frac{1}{2} \rho_\alpha(T) = \frac{1}{2} \frac{[A]K_0 \exp(\Delta H/RT)}{[A]K_0 \exp(\Delta H/RT) + 1}. \quad (9)$$

Taking into account Eq. (1) the functional behavior of the elastic constant G'_N beyond the gel point is expressed by a power law

$$G'_N(T) \sim [p(T) - p_c]^\gamma \quad [p(T) > p_c], \quad (10)$$

where p is the fraction of reacted bonds.

The equilibrium constant K_0 has been measured by several groups (e.g., [11,31,42,43]). One method is based on the measurement of the on-rates k_+ and off-rates k_- of the actin- α -actinin binding [31]. For rabbit smooth muscle α -actinin at 20 °C the kinetic constants $k_+ = 1.0 \times 10^6 \text{ mol}^{-1} \text{ s}^{-1}$ and $k_- = 0.4 \text{ s}^{-1}$ were found thus yielding

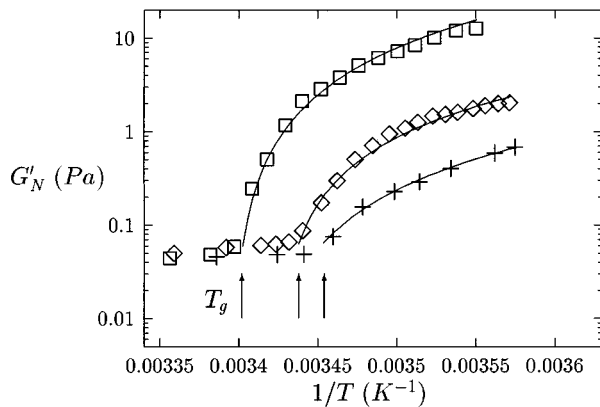


FIG. 6. Simulation of Arrhenius-like plots of elastic constant G'_N in terms of percolation model assuming chemical equilibrium for reacted crosslinkers [Eq. (9)]. The actin- α -actinin molar ratios were (+) $r_{A\alpha}=27$, (\diamond) $r_{A\alpha}=20$, and (\square) $r_{A\alpha}=10$. For $r_{A\alpha}=55$ no fit was done because of the small number of available data points; see Fig. 3. Lines: fitted power laws for temperatures below the gel point temperature $1/T > 1/T_g$ (for values of $1/T_g$ see Table I). The fits were done with nearly the same values of free parameters $\Delta H=1.6$ – 2.9 kJ, $p_c=0.44$ – 0.47 , and exponent $\gamma=1.5$ – 1.8 .

$$K_0 = \frac{k_+}{k_-} = 0.4 \times 10^6 \text{ mol}^{-1}.$$

Our experiments were performed at the actin concentration $c_A \equiv [A] = 9.5 \mu\text{mol}$ where $[A]K_0 = 3.8$.

Using the percolation relation Eq. (10) and the above value for the product $[A]K_0$ we simulated the G'_N versus $1/T$ curves shown in Fig. 3. Only data points at temperatures $1/T > 1/T_g$ were considered. The results of the data fitting are presented in Fig. 6, where the lines present the percolation model. A reasonably good agreement between the experimental data and the fitted model function is observed for actin- α -actinin ratios $r_{A\alpha} = 10, 20$, and 27 while for $r_{A\alpha} = 55$ the number of data points was too small to fit the data. All curves were fitted with nearly the same values of the free parameters $\Delta H=1.6$ – 2.9 kJ, $\gamma=1.5$ – 1.8 , and $p_c=0.44$ – 0.47 . The value of the critical exponent $\gamma=1.5$ – 1.8 agrees rather well with the mean field value, $t=1.7$ – 1.9 [36], but not with the value predicted for three-dimensional percolation networks $t \approx 3.8$ [44]. However, if only the initial slope of the data points near the gel point is considered, a value of $\gamma=3.6$ – 4.0 is found.

Characterization of the gel point. Gel formation is expected to be associated with phase separation if the volume density of cross-links formed is larger than the density of entanglement points. Or in other words, if the average distance d_{cc} between randomly distributed cross-links on a filament becomes smaller than the mesh size ξ . If we assume a cubic lattice of the entangled solution the number of sides to the number of entanglement points is 3:1. The number of actin monomers (diameter $a \approx 5.5$ nm [45]) per side of length ξ of the lattice is $n_A = 2\xi/a$ (the double stranded structure of F -actin is taken into account by the factor 2). Thus the limiting value of the actin-to-cross-linker ratio \hat{r}_{AC} where all points of entanglement are fixed, is approximately given by

$$\hat{r}_{AC} = \frac{3}{2} n_A = 3 \frac{\xi}{a}. \quad (11)$$

We define \hat{r}_{AC} as the apparent gel point of our network.

A number of cross-linkers exhibit much larger association equilibrium constants K_0 than α -actinin and do not dissociate below physiological temperatures. Examples are filamin and 30 kDa cross-linker from *Dictyostelium discoideum*. In separate experiments (unpublished data) we found that for the two latter types of cross-linkers and an actin concentration of $c_A = 7.0 \mu\text{mol}$ (mesh size $\xi = 0.64 \mu\text{m}$) the gel point is observed at $\hat{r}_{AC} \approx 500$. Since both molecules are bivalent cross-linkers one expects from Eq. (11) an actin-cross-linker ratio of $\hat{r}_{AC} \approx 350$, in good agreement with the experimentally observed \hat{r}_{AC} value.

The above consideration shows that the gel point for actin- α -actinin networks is expected at considerably lower $r_{A\alpha}$ values in correspondence with our experimental data.

According to Table I the gel point temperature T_g increases linearly with decreasing actin- α -actinin ratio ($r_{A\alpha}/T_g \approx \text{const}$) at constant actin concentration. This displacement law can be rationalized in terms of the kinetic model as follows:

For constant actin concentrations the gel point always occurs at the same effective value of the actin- α -actinin ratio $r_{A\alpha}^{\text{eff},g}(T)$. It depends on the fraction of cross-linker molecules reacted $\rho_\alpha(T)$ according to

$$r_{A\alpha}^{\text{eff},g}(T) = \frac{r_{A\alpha}}{\rho_\alpha(T)}. \quad (12)$$

The temperature dependence of $\rho_\alpha(T)^{-1}$ is approximately determined by the linear term of a Taylor expansion in terms of $(1/T - 1/T_0)$, and the effective actin- α -actinin ratio is of the form

$$r_{A\alpha}^{\text{eff}} = r_{A\alpha} \left[\rho_\alpha(T_0)^{-1} + \text{const} \left(\frac{1}{T} - \frac{1}{T_0} \right) + \dots \right].$$

Since the gel point at constant actin concentration is determined by a unique value of $r_{A\alpha}^{\text{eff}}$ the following condition must hold:

$$r_{A\alpha}/T_g \approx \text{const},$$

which is the experimentally found displacement law.

It is important to note that the actual position of the gel point may be shifted with respect to the value of T_g , defined in Fig. 2. As has been pointed out by various groups [46–49], the characteristic length of the entangled network is not the mesh size ξ but the entanglement length ξ_e , which may be considerably larger than ξ unless the end-to-end distance of the filaments is an order of magnitude larger than the mesh size [46]. In our experiments the actin concentration was $c_A = 9.5 \mu\text{mol}$, which corresponds to a mesh size of $\xi \approx 0.55 \mu\text{m}$, and the chain length was adjusted by gelsolin to about $22 \mu\text{m}$ ($r_{AG} = 8000$). Thus the shift of T_g is expected to be small.

Phase diagram of microgelation and bundle formation. At increasing degree of cross-linking the formation of three types of structures can be observed: (1) a homogeneous gel,

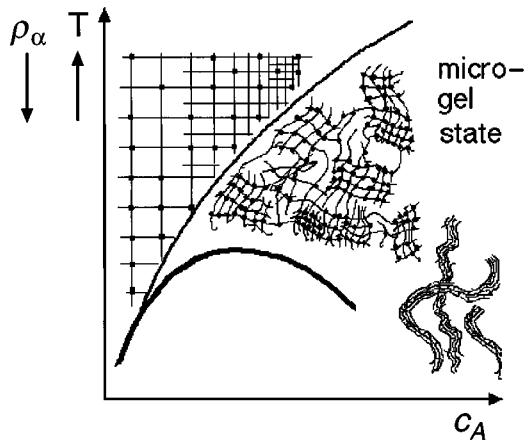


FIG. 7. Equivalent phase diagram of actin- α -actinin network. As abscissa the actin molar fraction or the mesh size can be used since $\xi \sim c_A^{1/2}$. As ordinate the temperature T or the fraction of reacted cross-linkers ρ_α could be taken. Note that decreasing values of ρ_α correspond to increasing values of T . The thin line defines the phase boundary of the sol-gel percolation transition. Above this line the mesh size of the network is not changed by cross-linking. Below the line the mesh size strongly fluctuates but the gel remains macroscopically homogeneous. In the vertical direction the fluctuations become more pronounced with increasing fraction of reacted bonds. The thick boundary defines the miscibility gap below which bundles of actin filaments coexist with highly dilute solutions of actin filaments.

(2) a locally heterogeneous but macroscopically homogeneous microgel, and (3) a coexistence of sol and gel consisting of bundles.

In the following we attempt to represent the sol-gel transition, the microgelation, and the bundle formation in terms of a ρ_α - c_A -phase diagram similar to the equivalent phase diagram proposed by deGennes for synthetic gels [36]. The phase diagram is presented in Fig. 7. Since the fraction of cross-linkers reacted increases with decreasing temperature, the ordinate could also be represented by a temperature scale with increasing values of T pointing in the positive y direction.

The thin line in Fig. 7 defines the phase boundary of the gel point. Above this line the cross-linkers are expected to connect the points of entanglement of the actin solution without appreciably changing the equilibrium mesh size. In this regime the distance between cross-linker d_{cc} is greater than the mesh size ξ . According to Fig. 2 and previous studies [19] the elastic modulus G'_N increases only slightly while the viscosity η diverges. Exactly the same behavior was found for other much stronger cross-linkers as filamin and 120 kDa cross-linker from *Dictyostelium discoideum* cells (unpublished data).

Below the phase line of the gel point local mesh size fluctuations arise because d_{cc} becomes smaller than the average value of ξ and cross-linking is associated with local contractions of the meshwork. However, since the filament length is large compared to ξ the network remains homogeneous on a macroscopic scale.

When further increasing the fraction of bonds reacted, the fluctuations in polymer density (or the coarseness of the microgel) become more and more pronounced. The clusters

separate completely and macroscopic phase separation into a sol and a tightly packed gel occurs. The latter consists mainly of parallel bundles of cross-linked gel. The coexistence between bundles and sol is described by a miscibility gap (Fig. 7, thick line) but nothing is yet known about the phase line and the critical point. The situation in this phase regime is complicated by pronounced kinetic effects since the bundle formation is strongly hindered in random networks of long filaments. We found out in separate experiments that the development of bundles can already be observed at $r_{A\alpha} = 50$ if the network is annealed for 5 days at 4 °C. Annealing only one day under the same conditions a bundling threshold of $r_{A\alpha} < 5$ is found.

V. BIOLOGICAL IMPLICATIONS

The present work shows that gelation of networks of semiflexible actin filaments passes through the same sequence of transitions at increasing degrees of cross-linking as synthetic gels [36]: from a homogeneous, partially cross-linked network to a macroscopically homogeneous microphase and finally into a state of sol-gel coexistence where the gel consists of bundles. Since bundle formation is also induced by other cross-linkers (notably filamin) we postulate that the behavior found for α -actinin is universal for all actin-cross-linker networks.

The formation of bundles, however, is strongly impeded in networks composed of long filaments (contour length of filaments is large compared to mesh size ξ) but occurs much more readily for filament lengths comparable to ξ [50]. In biological cells such as *Dictyostelium discoideum*, 80% of the actin filaments have lengths of the order of 0.5 μm and only 10% exhibit μm lengths [51]. Therefore in such cells bundling is highly probable.

Another intriguing question is whether α -actinin can actually form cross-links in cells at physiological temperatures since the constant K of the association-dissociation equilibrium is rather small and the gel point temperature is low. On the other side we found a displacement law showing that the gel point is strongly shifted to higher temperatures with a decreasing actin-cross-linker ratio.

In cells the actin concentration is much higher (about an order of magnitude) than in our *in vitro* models and the actin- α -actinin ratio is $r_{A\alpha} \approx 80$ for the case of *Dictyostelium discoideum* cells [52]. According to Eq. (9) the temperature of the midpoint of the reaction—where $\rho_\alpha = 1/2$ —is determined by the condition

$$[A]K_0 \exp(\Delta H/RT) = 1.$$

Since $\Delta H \approx RT$ an increase of $[A]$ by a factor of 10 would increase the absolute temperature of the midpoint by about a factor of two (that is from 300 K to 600 K). In cells the dissociation-association equilibrium of the actin- α -actinin system is easily shifted to the side of association by adjustment of the fraction of polymerizable actin controlled by the sequestering actin-binding protein profilin [25]. The sensitive dependence of the gel point on the actin concentration and

the actin-to- α -actinin ratio provides cells with a powerful tool to control the elasticity of the actin-based cytoskeleton, in particular if the parameters $[A]$ and $r_{A\alpha}$ of the actin network are adjusted nearly to a phase boundary.

ACKNOWLEDGMENTS

First of all we would like to thank Mrs. I. Sprenger for the preparation of excellent electron micrographs and Mrs. H.

Hirsch, Mrs. H. Kirpal, and Mrs. K. Scharpf for isolation and purification of protein. Helpful discussion with K. Kremer is gratefully acknowledged. Secondly, we greatly appreciate continuous and enlightening discussions with E. Frey and K. Kroy of the Department of Physics. For careful reading of this manuscript we thank Ms. C. Meissner. This work was supported by the Deutsche Forschungsgemeinschaft (SFB 266) and the Fonds der Chemischen Industrie.

-
- [1] S. K. Maciver, *Microfilament Organization and Actin Binding Proteins in The Cytoskeleton*, Vol. 1, *Structure and Assembly*, edited by J. E. Hesketh and I. Pryme (JAI, Greenwich, 1995), p. 1.
- [2] E. Evans, A. Leung, and D. Zhelev, *J. Cell Biol.* **122**, 1295 (1993).
- [3] J. Condeelis, *Annu. Rev. Cell Biol.* **9**, 411 (1993).
- [4] E. D. Korn, *Physiol. Rev.* **62**, 672 (1982).
- [5] A. Wegner, *J. Mol. Biol.* **108**, 139 (1976).
- [6] A. Wegner and G. Isenberg, *Proc. Natl. Acad. Sci. USA* **80**, 4922 (1983).
- [7] T. P. Stossel *et al.*, *Annu. Rev. Cell Biol.* **1**, 353 (1985).
- [8] J. H. Hartwig and D. J. Kwiatkowski, *Curr. Opin. Cell Biol.* **3**, 87 (1991).
- [9] P. A. Janmey, J. Peetermans, K. S. Zaner, T. P. Stossel, and T. Tanaka, *J. Biol. Chem.* **261**, 8357 (1986).
- [10] B. M. Jockusch and G. Isenberg, *Proc. Natl. Acad. Sci. USA* **78**, 3005 (1981).
- [11] D. H. Wachsstock, W. H. Schwartz, and T. D. Pollard, *Biophys. J.* **65**, 205 (1993).
- [12] S. Kaufmann, J. Käs, W. H. Goldmann, E. Sackmann, and G. Isenberg, *FEBS Lett.* **314**, 203 (1992).
- [13] J. Käs, H. Strey, J. X. Tang, D. Finger, R. Ezzell, E. Sackmann, and P. A. Janmey, *Biophys. J.* **70**, 609 (1996).
- [14] C. F. Schmidt, M. Bärmann, G. Isenberg, and E. Sackmann, *Macromolecules* **22**, 3638 (1989).
- [15] R. Götter, K. Kroy, E. Frey, M. Bärmann, and E. Sackmann, *Macromolecules* **29**, 30 (1996).
- [16] J. Käs, H. Strey, M. Bärmann, and E. Sackmann, *Europhys. Lett.* **21**, 865 (1993).
- [17] J. Käs, H. Strey, and E. Sackmann, *Nature* **368**, 226 (1994).
- [18] M. Sato, W. H. Schwarz, and T. D. Pollard, *Nature* **325**, 828 (1987).
- [19] O. Müller, H. E. Gaub, M. Bärmann, and E. Sackmann, *Macromolecules* **24**, 3111 (1991).
- [20] R. Ruddies, W. H. Goldmann, G. Isenberg, and E. Sackmann, *Eur. Biophys. J.* **22**, 309 (1993).
- [21] D. H. Wachsstock, W. H. Schwartz, and T. D. Pollard, *Biophys. J.* **66**, 801 (1994).
- [22] J. M. Pardee and J. A. Spudich, *Methods Enzymol.* **85**, 164 (1982).
- [23] S. MacLean-Fletcher, and T. D. Pollard, *Biophys. Biochem. Res. Commun.* **96**, 18 (1980).
- [24] S. S. Lehrer and G. Kerwar, *Biochemistry* **72**, 1211 (1972).
- [25] T. D. Pollard and J. A. Cooper, *Annu. Rev. Biochem.* **55**, 987 (1986).
- [26] S. W. Craig, C. L. Lancashire, and J. A. Cooper, *Methods Enzymol.* **85**, 316 (1982).
- [27] J. A. Cooper, J. Bryan, B. Schwab III, C. Frieden, D. J. Loftus, and E. L. Elson, *J. Cell Biol.* **104**, 491 (1987).
- [28] M. M. Bradford, *Ann. Biochem.* **72**, 248 (1976).
- [29] U. K. Laemmli, *Nature* **227**, 680 (1970).
- [30] J. D. Ferry, *Viscoelastic Properties of Polymers* (Wiley, London, 1980).
- [31] W. H. Goldmann and G. Isenberg, *FEBS Lett.* **336**, 408 (1993).
- [32] P. A. Janmey, S. Hvidt, J. Lamb, and T. P. Stossel, *Nature* **345**, 89 (1990).
- [33] P. A. Janmey, S. Hvidt, J. Käs, D. Lerche, A. Maggs, E. Sackmann, M. Schliwa, and T. P. Stossel, *J. Biol. Chem.* **269**, 32503 (1994).
- [34] E. Sackmann, *Macromol. Chem. Phys.* **195**, 7 (1994).
- [35] E. D. Korn, M. F. Carlier, and D. Pantaloni, *Science* **238**, 638 (1987).
- [36] P.-G. deGennes, *Scaling Concepts in Polymer Physics* (Cornell University Press, Ithaca, 1979).
- [37] J. Bastide, L. Leibler, and J. Prost, *Macromolecules* **23**, 1821 (1990).
- [38] J. Bastide, E. Mendes, F. Boué, and M. Buzier, *Macromol. Chem. Macromol. Symp.* **40**, 81 (1990).
- [39] R. H. Colby, J. R. Gillmor, and M. Rubinstein, *Phys. Rev. E* **48**, 3712 (1993).
- [40] S. Arbabi and M. Sahimi, *Phys. Rev. Lett.* **65**, 725 (1990).
- [41] D. Stauffer and A. Aharony, *Introduction to Percolation Theory* (Taylor & Francis, London, 1992).
- [42] R. K. Meyer and U. Aebi, *J. Cell Biol.* **110**, 2013 (1990).
- [43] P. A. Kuhlman, J. Ellis, D. R. Critchley, and C. R. Bagshaw, *FEBS Lett.* **339**, 297 (1994).
- [44] S. Arbabi and M. Sahimi, *Phys. Rev. B* **38**, 7173 (1988).
- [45] W. Kabsch, H. G. Mannherz, and D. Suck, *EMBO J.* **4**, 2113 (1985).
- [46] T. A. Kavassalis and J. Noolandi, *Phys. Rev. Lett.* **59**, 2674 (1987); *Macromolecules* **21**, 2869 (1988); **22**, 2709 (1989).
- [47] E. R. Duering, K. Kremer, and G. S. Grest, *Phys. Rev. Lett.* **67**, 3531 (1991).
- [48] F. C. MacKintosh, J. Käs, and P. A. Janmey, *Phys. Rev. Lett.* **75**, 4425 (1995).
- [49] E. Frey and K. Kroy (private communication).
- [50] J. D. Cortese and C. Frieden, *J. Cell Biol.* **107**, 1477 (1988).
- [51] J. L. Podolski and T. L. Steck, *J. Biol. Chem.* **265**, 1312 (1990).
- [52] M. Schleicher (private communication).